

# Impairment of Skin Wound Healing in $\beta$ -1,4-Galactosyltransferase-Deficient Mice with Reduced Leukocyte Recruitment

Ryoichi Mori,\* Toshikazu Kondo,\*<sup>†</sup>  
Toshikazu Nishie,<sup>‡</sup> Tohru Ohshima,\* and  
Masahide Asano<sup>‡</sup>

From the Department of Forensic and Social Environmental Medicine,\* Graduate School of Medical Science, and the Division of Transgenic Animal Science,<sup>‡</sup> Advanced Science Research Center, Kanazawa University, Kanazawa; and the Department of Legal Medicine,<sup>†</sup> Wakayama Medical University, Wakayama, Japan

**Cell-surface carbohydrate chains are known to contribute to cell migration, interactions, and proliferation, but their roles in skin wound healing have not been evaluated. We examined the biological roles of  $\beta$ 4-galactosylated carbohydrate chains in skin wound healing using mutant mice that lack  $\beta$ -1,4-galactosyltransferase-I ( $\beta$ 4GalT-I), which is responsible for the biosynthesis of the type 2 chain in *N*-glycans and the core 2 branch in *O*-glycans.  $\beta$ 4GalT-I-deficient mice showed significantly delayed wound healing with reduced re-epithelialization, collagen synthesis, and angiogenesis, compared with control mice. Neutrophil and macrophage recruitment at wound sites was also impaired in these mice probably because of selectin-ligand deficiency. In accordance with the reduced leukocyte infiltration, the expression levels of macrophage-derived chemokines, transforming growth factor- $\beta$ 1, and vascular endothelial growth factor were all reduced in  $\beta$ 4GalT-I<sup>-/-</sup> mice. These results demonstrate that  $\beta$ 4-galactosylated carbohydrate chains play a critical role in skin wound healing by mediating leukocyte infiltration and epidermal cell growth, which affects the production of chemokines and growth factors. This study introduces a suitable mouse model for investigating the molecular mechanisms of skin wound healing and is the first report showing that carbohydrate chains have a strong influence on skin wound healing. (*Am J Pathol* 2004, 164:1303–1314)**

Wound healing immediately starts after an injury and proceeds with a complicated but well-organized interaction among various types of tissues and cells. Skin wound healing is composed of the inflammatory, proliferative,

and maturation phases. In the inflammatory phase, the recruitment of leukocytes such as neutrophils and macrophages into the wound site is a hallmark. In the proliferative phase, the migration and proliferation of keratinocytes, fibroblasts, and endothelial cells result in re-epithelialization and tissue granulation. In the maturation phase, excess collagen in the wound site is degraded by several proteolytic enzymes, leading to the completion of tissue repair.<sup>1,2</sup> It is well known that biological substances such as cytokines, chemokines, and growth factors are closely involved in every phase of wound healing process.

Inflammatory cells that migrate into wound sites play important roles in wound healing. In the early inflammatory phase, neutrophils begin to accumulate at the wound site to defend against invading microbes by releasing oxygen radicals and secreting proinflammatory cytokines that probably serve as the earliest signal to activate fibroblasts and keratinocytes. Subsequently, macrophages, as a producer for a battery of cytokines, chemokines, and growth factors, dominantly migrate to the wound site after the neutrophil accumulation. These molecules play important roles in the control of leukocyte recruitment and effector function as well as in hematopoiesis, angiogenesis, and adaptive immunity.<sup>3–7</sup> For instance, we previously showed that tumor necrosis factor (TNF) 55-kd receptor (TNF-Rp55) and interleukin-6 are crucially involved in leukocyte recruitment in the inflammatory phase.<sup>8,9</sup> On the other hand, cell-cell and cell-matrix interactions through cell surface molecules, especially cell surface carbohydrates, are also involved in cell adhesion, migration, and proliferation. Although the roles of cytokines, chemokines, and growth factors in the wound-healing process have been well studied, little is known about the involvement of cell-surface carbohydrates in skin wound healing.

$\beta$ -1,4-galactosyltransferase ( $\beta$ 4GalT)-I is a glycosyltransferase that transfers galactose (Gal) from UDP-Gal to the terminal *N*-acetylglucosamine (GlcNAc) of carbo-

Supported by the Ministry of Education, Culture, Sports, Science, and Technology of Japan (grants 13470101 and 13480280).

Accepted for publication December 22, 2003.

Address reprint requests to Masahide Asano, Ph.D., Division of Transgenic Animal Science, Advanced Science Research Center, Kanazawa University, 13-1 Takara-machi, Kanazawa 920-8640, Japan. E-mail: asano@kiea.m.kanazawa-u.ac.jp.

hydrate chains in a  $\beta$ 1,4-linkage to form a Gal $\beta$ 1 $\rightarrow$ 4GlcNAc structure in the Golgi apparatus. Although seven  $\beta$ 4GalT genes ( $\beta$ 4GalT-I to  $\beta$ 4GalT-VII) have been isolated so far,<sup>10,11</sup> the role of any individual  $\beta$ 4GalT protein is poorly understood.  $\beta$ 4GalTs are responsible for the biosynthesis of the type 2 chain in *N*-glycans and the core 2 branch in *O*-glycans. A variety of terminal carbohydrate epitopes such as Lewis x ( $Le^x$ ), Lewis a, and sialyl  $Le^x$  (s $Le^x$ ) are formed on these *N*- and *O*-glycans. These modified epitopes have important roles in cell-cell and cell-matrix interactions. For example, s $Le^x$  is a ligand for E- and P-selectins, which mediate the interaction between leukocytes and vascular endothelium as well as platelet cells.<sup>12,13</sup> To further elucidate the biological relevance of  $\beta$ 4-galactosylated carbohydrate chains,  $\beta$ 4GalT-I-deficient ( $\beta$ 4GalT-I<sup>-/-</sup>) mice have been independently generated by us and another group.<sup>14,15</sup>  $\beta$ 4GalT-I<sup>-/-</sup> mice exhibit growth retardation, semilethality, hyperplasia of the skin and small intestine, and impaired differentiation of intestinal villus cells. These findings suggest that  $\beta$ 4-galactosylated carbohydrate chains regulate the proliferation and differentiation of epithelial cells.<sup>14</sup> Pituitary insufficiency is also suggested in  $\beta$ 4GalT-I<sup>-/-</sup> mice, probably owing to the agalactosylation of pituitary hormones.<sup>15</sup> Impaired binding of  $\beta$ 4GalT-I-deficient sperm to the ZP3 of eggs<sup>16</sup> and enhanced branching morphogenesis in the mammary glands of  $\beta$ 4GalT-I<sup>-/-</sup> mice have also been reported.<sup>17</sup> Furthermore, our recent studies have shown that  $\beta$ 4GalT-I plays a crucial role in the biosynthesis of selectin ligands such as s $Le^x$ . As a result, acute and chronic inflammatory responses are suppressed in  $\beta$ 4GalT-I<sup>-/-</sup> mice, and neutrophil infiltration at the inflammatory sites is primarily reduced.<sup>18</sup> Because mice deficient in both P- and E-selectins show markedly reduced recruitment of inflammatory cells and delayed wound closure, endothelial selectins play an important role in skin wound healing.<sup>19</sup> However, the role of  $\beta$ 4-galactosylated carbohydrate chains and carbohydrate selectin ligands in skin wound healing remain to be elucidated.

In the present study, we examined the biological relevance of  $\beta$ 4-galactosylated carbohydrate chains to skin wound healing using the  $\beta$ 4GalT-I<sup>-/-</sup> mice. Skin wound healing was significantly delayed in these mice. Neutrophil and macrophage recruitment at the wound site in the inflammatory phase was reduced probably because of the reduced expression of selectin ligands in the  $\beta$ 4GalT-I<sup>-/-</sup> mice compared with  $\beta$ 4GalT-I<sup>+/-</sup> mice. Re-epithelialization was also delayed in the  $\beta$ 4GalT-I<sup>-/-</sup> mice, along with reduced collagen synthesis and angiogenesis. In accordance with these observations, the expression levels of macrophage-derived chemokines and growth factors were also reduced. Our results clearly demonstrate that  $\beta$ 4-galactosylated carbohydrate chains regulate skin wound healing by mediating leukocyte recruitment and the subsequent production of chemokines and growth factors.

## Materials and Methods

### Animals

The generation of  $\beta$ 4GalT-I<sup>-/-</sup> mice on a mixed 129/Sv and C57BL/6 background was described previously.<sup>14</sup> Sex- and age-matched (2 to 4 months old) heterozygous littermates were used as controls in the following experiments. Although approximately half of the  $\beta$ 4GalT-I<sup>-/-</sup> mice died before weaning period because of growth retardation,<sup>14</sup> half of them survived to be used for the experiments. When survivors were able to eat pellets, they gained weight and grew normally as described previously.<sup>14</sup> The carbohydrate structures of the serum glycoproteins of  $\beta$ 4GalT-I<sup>+/+</sup> and  $\beta$ 4GalT-I<sup>+/-</sup> mice were indistinguishable,<sup>20</sup> and no overt phenotypes were observed in the  $\beta$ 4GalT-I<sup>+/-</sup> mice. All of the mice were kept under specific pathogen-free conditions in an environmentally controlled clean room at the Institute for Experimental Animals, Advanced Science Research Center, Kanazawa University. The experiments were conducted according to the Committee on Animal Experimentation of Kanazawa University, Takara-machi Campus.

### Wound Model

Skin wounds were prepared as described previously.<sup>8</sup> Briefly, mice were anesthetized by intraperitoneal administration of Nembutal (5  $\mu$ g/g body weight; Dainippon Pharmaceutical Co., Ltd., Osaka, Japan). After shaving the dorsal hair and cleaning the exposed skin with 70% ethanol, full-thickness excisional skin wounds of 4-mm diameter were made aseptically on either side of the dorsal midline using a 4-mm biopsy punch (Kai Industries, Tokyo, Japan). Usually, six wounds were made on the same animal. Each wound region was digitally photographed at the indicated time intervals, and the areas of the wounds were calculated by PhotoShop software, version 7.0 (Adobe Systems, San Jose, CA). Changes in the wound areas were expressed as the percentage of the initial wound areas. In some series of experiments, wounds and their surrounding area, including the scab and epithelial margins, were harvested with an 8-mm biopsy punch (Kai Industries) at the indicated time intervals after the mice were killed with an overdose of diethylether.

### Histology and Immunohistochemistry

Wound tissues were fixed overnight in 4% formaldehyde buffered with phosphate-buffered saline (PBS) (pH 7.2), and embedded in paraffin. Sections (4  $\mu$ m thick) were subjected to hematoxylin and eosin (H&E) staining or immunostaining. For immunohistochemistry, deparaffinized sections were treated with endogenous peroxidase blocking reagent (DAKO Cytomation A/S, Copenhagen, Denmark) and proteinase K (DAKO Cytomation A/S) for 6 minutes at room temperature. They were then incubated with rabbit anti-myeloperoxidase (MPO) polyclonal antibody (diluted 1:100; Neomarkers, Fremont,

CA), anti-mouse F4/80 monoclonal antibody (mAb) (diluted 1:200; Dainippon Pharmaceutical Co.), or rat anti-mouse CD31 (platelet endothelial cell adhesion molecule 1) mAb (diluted 1:200; PharMingen, San Diego, CA) overnight at 4°C. The antibodies were appropriately diluted in antibody diluent with background-reducing components (DAKO Cytomation A/S). The sections reacted with anti-MPO antibody were stained with EnVision+ (DAKO Cytomation A/S) according to the manufacturer's instructions. The sections that had been reacted with anti-F4/80 and anti-CD31 antibodies were incubated with biotinylated rabbit anti-rat immunoglobulin (DAKO Cytomation A/S) for 1 hour at 37°C. The signals on the positive cells were then enhanced using the Catalyzed Signal Amplification System (DAKO Cytomation A/S) according to the manufacturer's instruction. Thereafter, counterstaining was performed with methyl green.

### *Analysis of Re-Epithelialization*

The analysis of re-epithelialization was performed according to the procedure of Low and colleagues.<sup>21</sup> The width of the wound and the distance between the leading edge of the keratinocyte migration were measured on H&E-stained wound sections. The degree of re-epithelialization was calculated as follows: re-epithelialization (%) = [distance covered by epithelium]  $\times$  100/[distance between wound edges].

### *Detection of Proliferating Cells by Labeling with 5'-Bromo-2'-Deoxyuridine (BrdU)*

In another experiment, wounded mice were injected intraperitoneally with 20  $\mu$ l/g body weight of BrdU labeling reagent (Roche Diagnostics GmbH, Mannheim, Germany) 2 hours before the sacrifice. Wound tissues were fixed overnight in 4% formaldehyde buffered with PBS (pH 7.2), and embedded in paraffin. Deparaffinized sections (4  $\mu$ m thick) were treated with the Histomouse-Plus kits (Zymed Laboratories Inc., South San Francisco, CA) to reduce background signals according to the manufacturer's instructions. Sections were incubated overnight at 4°C with a solution of mouse anti-BrdU antibody and nucleases for DNA denaturation in PBS/glycerin (diluted 1:10; Roche Diagnostics GmbH). Positive signals were enhanced by the Catalyzed Signal Amplification System (DAKO Cytomation), followed by counterstaining with methyl green.

### *Measurement of BrdU-Positive Cells, Macrophage Recruitment, and Angiogenesis*

A blinded observer counted BrdU-positive cells in the epidermis and F4/80-positive macrophages in the wound bed (defined as the area surrounded by unwounded skin, fascia, regenerated epidermis, and eschar) in five random high-power ( $\times$ 200) fields of each immunohistochemically stained section, as described previously.<sup>21</sup> The neovascular areas (CD31-positive cells) were mea-

sured in the whole wound bed areas using the freehand drawing tool of the PhotoShop software, and the degree of vascularization was calculated as described previously<sup>21</sup>: vascularization (%) = [CD31-positive area]  $\times$  100/[total wound bed area].

### *MPO Assay*

The excised wound samples were homogenized in 400  $\mu$ l of PBS. The homogenates were frozen and thawed three times, and then the debris was removed by centrifugation at 15,000 rpm. The MPO activity in the supernatants was measured using a Sumilon peroxidase assay kit (Sumitomo Bekuraito, Tokyo, Japan) according to the manufacturer's instructions. MPO activity was calculated using commercial peroxidase (Sigma, St. Louis, MO) as a standard.

### *Fluorescence-Activated Cell Sorting (FACS)*

#### *Analysis*

Neutrophils infiltrated into the wound sites were prepared 24 hours after the injury as described with some modifications.<sup>22</sup> The wounded skin samples were incubated with 0.15% trypsin (Invitrogen Co., Ltd., Carlsbad, CA) and 50 U/ml of Dispase (Invitrogen Co., Ltd.) in Hanks' solution (Nissui Pharmaceutical Co., Ltd., Tokyo, Japan) for 1 hour at 37°C, and then stirred in PBS containing 0.15% DNase I for 1 hour at 37°C. Cell suspensions were centrifuged at 1500 rpm for 5 minutes at 4°C, and cells were incubated in 5 ml of hemolysis buffer (17 mmol/L Tris-HCl containing 140 mmol/L NH<sub>4</sub>Cl, pH 7.2) for 5 minutes at room temperature. Cells were washed with RPMI 1640 medium, resuspended in 1 ml of FACS solution (2% fetal calf serum and 0.01% azide in Hanks' solution), and filtrated through the nylon mesh.

Cells ( $1 \times 10^6$ ) were blocked with mouse Fc block (anti-mouse CD16/CD32, PharMingen) and goat serum for 15 minutes, and then washed with the FACS solution. Cells were incubated with mouse P-selectin fused to human IgG (P-selectin-hIgG) chimeric molecule (PharMingen) for 20 minutes. After washing, cells were incubated with fluorescein isothiocyanate-conjugated anti-mouse Ly-6G and Ly-6C (Gr-1) (PharMingen) and red macrophytic alage phycoerythrin (R-PE)-conjugated goat anti-human IgG (Jackson ImmunoResearch Laboratories, Inc., West Grove, PA) for 20 minutes. Incubations with antibodies were performed on ice. After washing, cells were applied to FACS analysis and neutrophil populations were gated by Gr-1. Data were analyzed on a FACSCalibur flow cytometer using CellQuest software (Becton Dickinson, Mountain View, CA).

### *Hydroxyproline (HP) Analysis*

The collagen content of the wound area was assessed by determining the amount of HP, a major component of collagen.<sup>23</sup> HP content was measured as described previously.<sup>24</sup> In brief, samples of skin tissue were dried at

**Table 1.** Sequences of the Primers Used for RT-PCR

Transcript	Sequence	Annealing temperature (°C)	Product length (bp)	Cycles
MCP-1	(F) 5'-ACTGAAGCCAGCTCTCTCTTCTC-3' (R) 5'-TTCCTTCTTGGGGTCAGCACAGAC-3'	60	274	25
MIP-1 $\alpha$	(F) 5'-GCCCTTGCTGTTCTTCTGT-3' (R) 5'-GGCAATCAGTTCCAGGTCAGT-3'	57	258	25
MIP-2	(F) 5'-GAACAAAGGCAAGGCTAACTGA-3' (R) 5'-AACATAACATCTGGGCAAT-3'	56	205	25
TGF- $\beta$ 1	(F) 5'-CGGGGCGACCTGGGCACCATCCATGAC-3' (R) 5'-CTGCTCCACCTTGGGCTTGCACCCAC-3'	60	405	35
TGF- $\alpha$	(F) 5'-ATGGTCCCCGCGACCGGACAGCTC-3' (R) 5'-ACATGCTGGCTTCTTCTTCTGCA-3'	60	190	35
COL1A1	(F) 5'-GCCAAGAAGACATCCCTGAAG-3' (R) 5'-TCATTGCATTGCACGTCATC-3'	60	139	40
VEGF	(F) 5'-TGAACCTTCTGCTCTCTTGG-3' (R) 5'-AACAAATGCTTCTCCGCTC-3'	60	457	35
$\beta$ -actin	(F) 5'-TTCTACAATGAGCTGCGTGTGGC-3' (R) 5'-CTCATAGCTCTTCTCCAGGGAGGA-3'	60	456	25

(F), Forward primer; (R), reverse primer.

120°C for 16 hours and then hydrolyzed in 2 ml of 6 N HCl at 100°C for 8 hours. Five hundred  $\mu$ l of citrate/acetate buffer (5% citric acid, 7.24% sodium acetate, 3.4% NaOH, 1.2% acetic acid) and 2 ml of chloramine T solution (1.13% chloramine T, 8% 1-propanol, 64% citrate/acetate buffer) were added to each sample, and the samples were incubated at room temperature for 20 minutes. Two ml of Ehrlich's solution (10.13 g of *p*-dimethylaminobenzaldehyde, 41.85 ml of 1-propanol, 17.55 ml of 70% perchloric acid) was then added, and the resulting mixture was incubated at 65°C for 20 minutes. The samples were cooled with cold tap water for 10 minutes. Absorbance at 550 nm was measured, and the amount of HP was determined by comparison to a standard curve. All of the reagents used in this assay were purchased from Wako Co., Osaka, Japan.

### RNA Isolation and Semiquantitative Reverse Transcriptase-Polymerase Chain Reaction (RT-PCR) Analysis

Total RNA was extracted from untreated and skin wound samples using Isogen (Nippon Gene Co., Ltd., Toyama, Japan), according to the manufacturer's instructions. Ten  $\mu$ g of total RNA was reverse-transcribed into cDNA using the SuperScript first-strand synthesis system for RT-PCR (Invitrogen Corp., Carlsbad, CA). Semiquantitative RT-PCR was performed according to the published method.<sup>25,26</sup> The synthesized cDNA was amplified using TaqDNA polymerase (Nippon Gene Co., Ltd.) and specific primers for target genes. Amplification was performed in a GeneAmp PCR System 9700 (Applied Biosystems, Foster City, CA). The optimum number of amplification cycles to obtain quantitative results was determined for each gene by testing at intervals of five cycles; each cycle included denaturation at 94°C for 30 seconds, annealing at 60°C for 30 seconds, extension at 72°C for 1 minute, and a final extension for 5 minutes, after which the sample was cooled to 4°C. The primer sequences, cycle numbers, and product sizes are de-

scribed in Table 1. The PCR products were separated by electrophoresis on a 2% agarose gel and stained with ethidium bromide. The density of the DNA bands was analyzed by NIH Image version 1.62 software (National Institutes of Health, Bethesda, MD) and compared with that of  $\beta$ -actin bands to quantify the PCR products.

### Enzyme-Linked Immunosorbent Assay (ELISA)

Samples of wounded skin were homogenized in 300  $\mu$ l of lysis buffer (10 mmol/L PBS, 0.1% sodium dodecyl sulfate, 1% Nonidet P-40, 5 mmol/L ethylenediaminetetraacetic acid) (EDTA) containing Complete protease inhibitor mixture (Roche Diagnostics GmbH) to extract the proteins. The homogenates were centrifuged at 15,000 rpm for 15 minutes at 4°C to remove the debris. The MIP-1 $\alpha$ , MIP-2, MCP-1, transforming growth factor (TGF)- $\beta$ 1, and vascular endothelial growth factor (VEGF) protein contents in the supernatant were measured with an ELISA kit (Quantikine M; R&D Systems, Inc., Minneapolis, MN) according to the manufacturer's instructions. The total protein concentration was measured with a BCA protein assay reagent kit (Pierce Biotechnology, Inc., Rockford, IL). The data were expressed as cytokine or growth factor/total protein (pg/mg) for each sample.

### Statistical Analysis

Statistical differences were determined using the Mann-Whitney *U*-test or analysis of variance. All data are presented as the mean  $\pm$  SEM. A *P* value <0.05 was accepted as statistically significant.

## Results

### Impairment of Skin Wound Healing in $\beta$ 4GalT-I-Deficient Mice

To elucidate the role of carbohydrate chains in the wound-healing process, we made full-thickness exci-



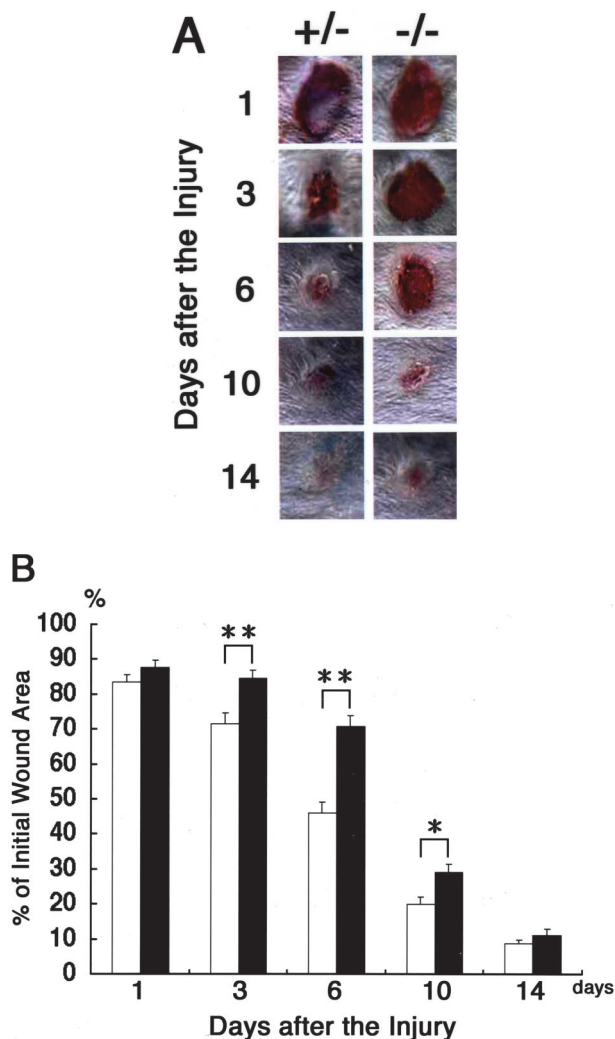


**Figure 1.** Skin wound healing in  $\beta 4\text{GalT-I}^{+/+}$  and  $\beta 4\text{GalT-I}^{-/-}$  mice. **A:** Macroscopic observation of wounds in  $\beta 4\text{GalT-I}^{+/+}$  and  $\beta 4\text{GalT-I}^{-/-}$  mice. Wounds were photographed from the same distance at the indicated time after the injury. Representative results of the six animals in each group are shown. **B:** The ratio of the wound area to the initial wound area at each time point after the injury in  $\beta 4\text{GalT-I}^{+/+}$  (open bars) and  $\beta 4\text{GalT-I}^{-/-}$  (filled bars) mice. Data are expressed as the mean  $\pm$  SEM ( $n = 6$ ). \*,  $P < 0.05$ ; \*\*,  $P < 0.01$ .

sional wounds on the dorsal skin of  $\beta 4\text{GalT-I}^{-/-}$  mice and their  $\beta 4\text{GalT-I}^{+/+}$  littermates (as controls), and the wound-healing process was monitored (Figure 1A). One day after the injury, the wound sites of the  $\beta 4\text{GalT-I}^{-/-}$  mice were similar in size and appearance to those of the  $\beta 4\text{GalT-I}^{+/+}$  mice. Three days after the injury, however, wound closure in the  $\beta 4\text{GalT-I}^{-/-}$  mice was markedly delayed compared with that of the  $\beta 4\text{GalT-I}^{+/+}$  mice (82% in  $\beta 4\text{GalT-I}^{-/-}$  mice versus 68% in  $\beta 4\text{GalT-I}^{+/+}$  mice,  $P < 0.01$ ) (Figure 1B). Thereafter, the wound areas of the  $\beta 4\text{GalT-I}^{-/-}$  mice remained significantly larger than those of the  $\beta 4\text{GalT-I}^{+/+}$  mice, but finally, 14 days after the injury, the wounds of the  $\beta 4\text{GalT-I}^{-/-}$  mice healed to the same degree as those of the  $\beta 4\text{GalT-I}^{+/+}$  mice (Figure 1B). These results indicate that macroscopic wound healing was delayed in  $\beta 4\text{GalT-I}^{-/-}$  mice.

### Delayed Re-Epithelialization at the Wound Sites of $\beta 4\text{GalT-I}$ -Deficient Mice

During the wound-healing process, re-epithelialization is one of the crucial events. Thick and hyperproliferative epithelia as well as extensive granulated tissues form to cover the wound. We compared the re-epithelialization of the wounds of the  $\beta 4\text{GalT-I}^{+/+}$  and  $\beta 4\text{GalT-I}^{-/-}$  mice (Figure 2). One day after the injury, no re-epithelialization was observed in either mouse (Figure 2G). The rate of re-epithelialization in the wounds of the  $\beta 4\text{GalT-I}^{-/-}$  mice was significantly lower on days 3 and 6 after the injury than in those of the  $\beta 4\text{GalT-I}^{+/+}$  mice (Figure 2G). Immunohistochemical analysis on proliferating cells with BrdU demonstrated that the number of BrdU-positive cells in the  $\beta 4\text{GalT-I}^{-/-}$  wounds was also significantly lower at 6 days after the injury than in the  $\beta 4\text{GalT-I}^{+/+}$  wounds (Figure 3; A to C).

RT-PCR analysis failed to detect any mRNA of TGF- $\alpha$  in uninjured skin samples derived from both mice. After the injury, the gene expression was dramatically increased 3 and 6 days in the  $\beta 4\text{GalT-I}^{+/+}$  mice, while the induction levels were less in the  $\beta 4\text{GalT-I}^{-/-}$  mice (Figure 3, D and E). These results are consistent with the macroscopic observations, and suggest that  $\beta 4\text{GalT-I}$  deficiency delayed re-epithelialization in skin wound healing.

### Reduced MPO Activity and Macrophage Infiltration at the Wound Sites of $\beta 4\text{GalT-I}$ -Deficient Mice

A variety of leukocytes migrate outside blood vessels and infiltrate into the wound site during the wound-healing process; the specific cell type(s) depends on the type of wound and the time after the injury. In the inflammatory phase, neutrophils and macrophages are the main infiltrates in the wound site. In  $\beta 4\text{GalT-I}^{+/+}$  mice, a large number of neutrophils were detected immunohistochemically 24 hours after the injury using the anti-MPO antibody (Figure 4, A and B). In contrast, neutrophil infiltration at the wound sites in  $\beta 4\text{GalT-I}^{-/-}$  mice was markedly lower than at those of the  $\beta 4\text{GalT-I}^{+/+}$  mice (Figure 4, C and D). Moreover, we measured the MPO activity to evaluate the neutrophil recruitment at the wound site. The MPO activity was significantly lower in the  $\beta 4\text{GalT-I}^{-/-}$  wound sites 6 hours and 24 hours after the injury compared with the  $\beta 4\text{GalT-I}^{+/+}$  wound sites (Figure 4E).

The number of infiltrated macrophages at wound sites was examined using the anti-F4/80 antibody, which recognizes mature macrophages (Figure 5; A to D).<sup>27</sup> Infiltration of F4/80-positive macrophages into wound sites was observed 1 day after the injury and reached its maximum 6 days after the injury in the  $\beta 4\text{GalT-I}^{+/+}$  wound sites (Figure 5E). The number of F4/80-positive macrophages at the wound sites in  $\beta 4\text{GalT-I}^{-/-}$  mice was significantly lower 3 and 6 days after the injury compared with the number in the  $\beta 4\text{GalT-I}^{+/+}$  wound sites, although it was comparable 1 day after the injury (Figure 5E). These results suggest that  $\beta 4\text{GalT-I}$  is involved in leukocyte recruitment in skin wound healing.

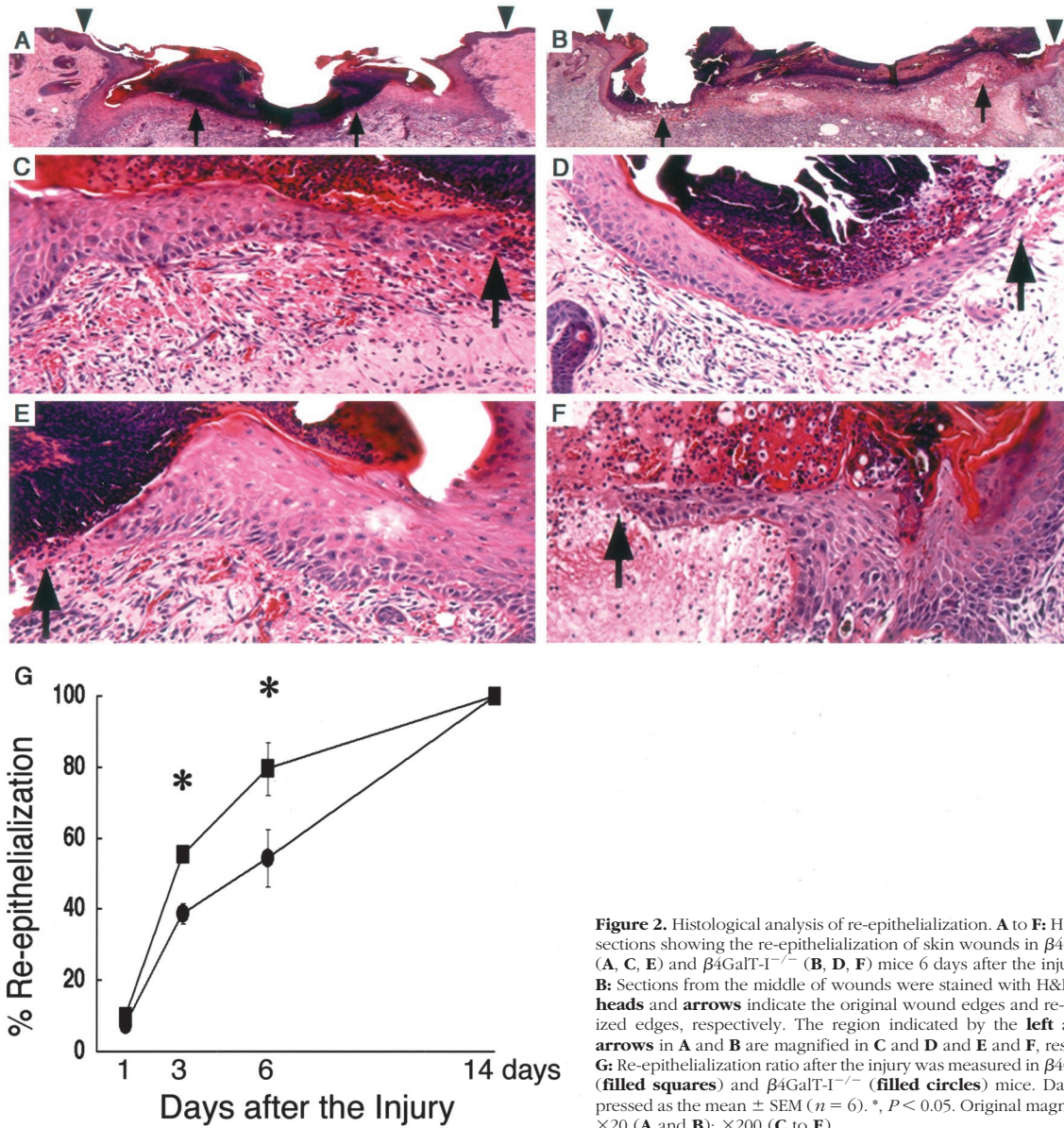


**Figure 2.** Histological analysis of re-epithelialization. **A to F:** Histological sections showing the re-epithelialization of skin wounds in  $\beta 4\text{GalT-1}^{+/+}$  (**A, C, E**) and  $\beta 4\text{GalT-1}^{-/-}$  (**B, D, F**) mice 6 days after the injury. **A and B:** Sections from the middle of wounds were stained with H&E. **Arrowheads and arrows** indicate the original wound edges and re-epithelialized edges, respectively. The region indicated by the **left and right arrows** in **A and B** are magnified in **C and D** and **E and F**, respectively. **G:** Re-epithelialization ratio after the injury was measured in  $\beta 4\text{GalT-1}^{+/+}$  (**filled squares**) and  $\beta 4\text{GalT-1}^{-/-}$  (**filled circles**) mice. Data are expressed as the mean  $\pm$  SEM ( $n = 6$ ). \*,  $P < 0.05$ . Original magnifications:  $\times 20$  (**A and B**);  $\times 200$  (**C to E**).

### Reduced Expression of Selectin Ligands on Infiltrated Neutrophils into the Wounds

We have previously shown that expression of P-selectin ligands on neutrophils and monocytes from the spleen of  $\beta 4\text{GalT-1}^{-/-}$  mice was reduced compared to control mice, indicating impaired biosynthesis of selectin ligands in  $\beta 4\text{GalT-1}^{-/-}$  mice.<sup>18</sup> Reduced infiltration of neutrophils and macrophages at the wound sites in  $\beta 4\text{GalT-1}^{-/-}$  mice could be caused by the same reason. To confirm this notion, FACS analysis using the P-selectin-hIgG chimeric molecule were performed. As shown in Figure 6, there were infiltrated neutrophils that bound the P-selectin-hIgG strongly in  $\beta 4\text{GalT-1}^{+/+}$  mice, whereas those from  $\beta 4\text{GalT-1}^{-/-}$  mice bound it weakly. Because nonspecific binding by the second antibody (goat PE-anti-human IgG) alone was detected in  $\beta 4\text{GalT-1}^{-/-}$  mice even in the

presence of normal goat serum, mean fluorescence intensities of specific binding were calculated by subtracting those of PE-anti-hIgG alone (filled histogram) from those of P-selectin-hIgG and PE-anti-hIgG (open histogram). Mean fluorescence intensities of specific binding (mean values  $\pm$  SEM) in  $\beta 4\text{GalT-1}^{-/-}$  mice ( $116.5 \pm 28.5$ ) were significantly lower than those in  $\beta 4\text{GalT-1}^{+/+}$  mice ( $225.2 \pm 22.4$ ) in three independent experiments (Student's *t*-test,  $P < 0.05$ ). In addition, specific binding through P-selectin and its ligands was confirmed by the reduction of binding to background levels in the presence of EDTA (data not shown). Therefore, the reduced infiltration of neutrophils and probably macrophages at the wound sites in  $\beta 4\text{GalT-1}^{-/-}$  mice was caused by the reduced expression of selectin ligands on these cells.



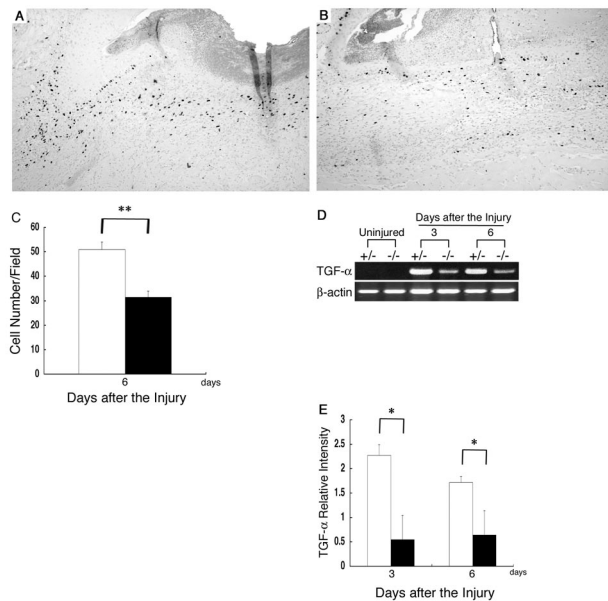


**Figure 3.** Proliferation of keratinocytes. **A** and **B**: Analysis of cell proliferation by immunohistochemical staining with the anti-BrdU monoclonal antibody in  $\beta 4\text{GalT-I}^{+/+}$  (**A**) and  $\beta 4\text{GalT-I}^{-/-}$  (**B**) mice 6 days after the injury. **C**: The number of anti-BrdU-positive cells per high-power microscopic field in the epidermis was counted. Data are expressed as the mean  $\pm$  SEM ( $n = 6$ ). \*\*,  $P < 0.01$ . **D**: RT-PCR analysis of the expression of the TGF- $\alpha$  gene at wound sites in  $\beta 4\text{GalT-I}^{+/+}$  and  $\beta 4\text{GalT-I}^{-/-}$  mice. RT-PCR analysis did not detect any TGF- $\alpha$  mRNA in uninjured skin samples from mice of either genotype. Representative results for the six animals in each group are shown. **E**: Relative expression levels of TGF- $\alpha$  normalized to  $\beta$ -actin mRNA levels in  $\beta 4\text{GalT-I}^{+/+}$  (open bars) and  $\beta 4\text{GalT-I}^{-/-}$  (filled bars) wound sites were determined by RT-PCR 3 and 6 days after the injury. Data are expressed as mean  $\pm$  SEM ( $n = 6$ ). \*,  $P < 0.05$ . Original magnifications:  $\times 100$  (**A**, **B**);  $\times 200$  (**C**).

### Reduced Expression of Chemokines at Wound Sites in $\beta 4\text{GalT-I}$ -Deficient Mice

To compare the expression levels of the chemokines at the wound sites of the  $\beta 4\text{GalT-I}^{+/+}$  and  $\beta 4\text{GalT-I}^{-/-}$  mice, semiquantitative RT-PCR was performed for MIP-1 $\alpha$ , MIP-2, and MCP-1 (Figure 7A). Under the used experimental condition, no mRNAs of these chemokines were detected in uninjured skin samples from mice of either genotype, but their expression was induced after the injury. The mRNA levels of these chemokines were significantly lower 3 days, but not 6 days, after the injury in the  $\beta 4\text{GalT-I}^{-/-}$  wound sites compared with the  $\beta 4\text{GalT-I}^{+/+}$  wound sites (Figure 7; B to D). The reduced gene expression of these chemokines in the  $\beta 4\text{GalT-I}^{-/-}$  wound sites was confirmed by the chemokine protein levels as determined by an ELISA assay (Figure 7; E to G). The amounts of these chemokines correlated well with their mRNA levels. These results indicate that the reduced infiltration of neutrophils and macrophages in  $\beta 4\text{GalT-I}^{-/-}$  mice was accompanied by diminished expression of these chemokines.

### Reduced Collagen Synthesis at Wound Sites in $\beta 4\text{GalT-I}$ -Deficient Mice

Collagen synthesis is induced at wound sites to heal the injury. To assess collagen synthesis, we measured the

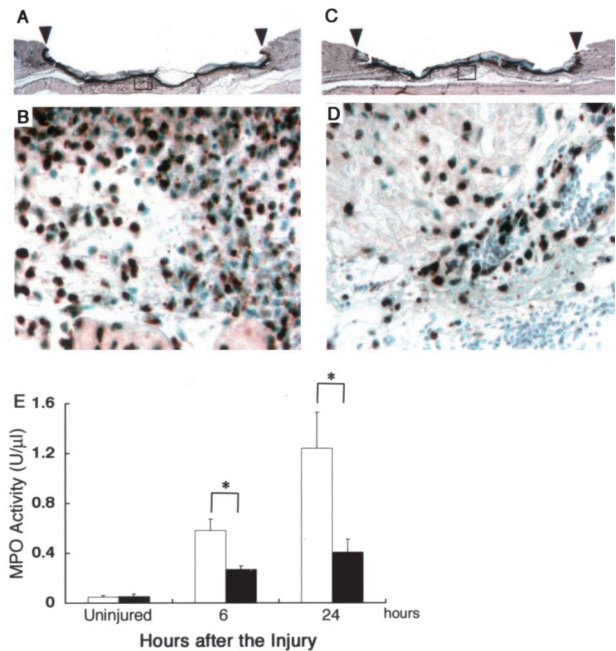


**Figure 4.** Neutrophil recruitment into wound sites. **A** to **D**: Neutrophil recruitment into skin wounds of  $\beta 4\text{GalT-I}^{+/+}$  (**A** and **B**) and  $\beta 4\text{GalT-I}^{-/-}$  (**C** and **D**) mice was analyzed using an anti-MPO antibody in samples taken 24 hours after the injury. **E**: MPO activity at the wound sites of  $\beta 4\text{GalT-I}^{+/+}$  (open bars) and  $\beta 4\text{GalT-I}^{-/-}$  (filled bars) mice 6 and 24 hours after the injury. Data are expressed as the mean  $\pm$  SEM ( $n = 6$ ). \*\*,  $P < 0.01$ . Original magnifications:  $\times 20$  (**A** and **C**);  $\times 200$  (**B** and **D**).

HP content at wound sites. The HP content was significantly lower 3 and 6 days after the injury in the  $\beta 4\text{GalT-I}^{-/-}$  wound sites compared with the  $\beta 4\text{GalT-I}^{+/+}$  wound sites (Figure 8A). The expression of the collagen type 1  $\alpha 1$  (COL1A1) gene was also examined by semiquantitative RT-PCR analysis (Figure 8B). Although RT-PCR analysis failed to detect any COL1A1 mRNA in uninjured skin samples from mice of either genotype, expression was induced after the injury. The level of COL1A1 mRNA was significantly lower in the  $\beta 4\text{GalT-I}^{-/-}$  wound sites 3 and 6 days after the injury compared with the  $\beta 4\text{GalT-I}^{+/+}$  wound sites (Figure 8C).

Because TGF- $\beta 1$  is known to induce the expression of COL1A1, the expression of TGF- $\beta 1$  was analyzed by semiquantitative RT-PCR (Figure 8B). Although RT-PCR analysis failed to detect any TGF- $\beta 1$  mRNA in uninjured skin samples from mice of either genotype, its expression was induced after the injury. As expected, both TGF- $\beta 1$  mRNA and its protein levels were significantly lower 3 and 6 days after the injury in the  $\beta 4\text{GalT-I}^{-/-}$  wound sites compared with the  $\beta 4\text{GalT-I}^{+/+}$  wound sites (Figure 8, D and E). The gene expression of connective tissue growth factor, which is induced by TGF- $\beta 1$ , was also significantly lower 3 and 6 days after the injury in the  $\beta 4\text{GalT-I}^{-/-}$  wound sites compared with the  $\beta 4\text{GalT-I}^{+/+}$  wound sites (data not shown). These observations indicate that reduced expressions of COL1A1 and TGF- $\beta 1$  are responsible for the diminished collagen accumulation at the wound sites of the  $\beta 4\text{GalT-I}^{-/-}$  mice.

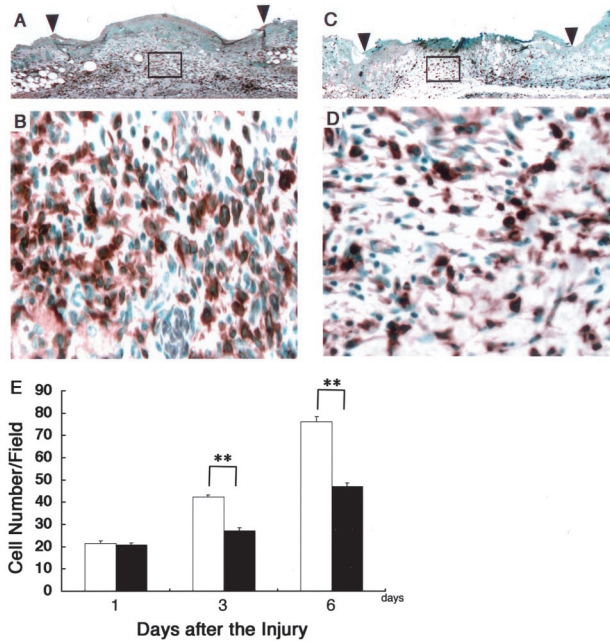


**Figure 5.** Macrophage recruitment into wound sites. **A to D:** Macrophage recruitment into skin wounds of  $\beta 4\text{GalT-I}^{+/+}$  (**A** and **B**) and  $\beta 4\text{GalT-I}^{-/-}$  (**C** and **D**) mice was analyzed using an anti-F4/80 antibody in samples taken 6 days after the injury. **E:** Macrophage recruitment into skin wounds of  $\beta 4\text{GalT-I}^{+/+}$  (open bars) and  $\beta 4\text{GalT-I}^{-/-}$  (filled bars) mice 1, 3, and 6 days after the injury. The number of recruited macrophages per high-power microscopic field was counted. Data are expressed as the mean  $\pm$  SEM ( $n = 12$ ). \*\*,  $P < 0.01$ . Original magnifications:  $\times 20$  (**A** and **C**);  $\times 200$  (**B** and **D**).

### Impaired Angiogenesis at Wound Sites in $\beta 4\text{GalT-I}$ -Deficient Mice

The neovascularization is indispensable for sustaining the newly formed granulated tissues in the wound-healing process. To compare the extent of angiogenesis between the  $\beta 4\text{GalT-I}^{+/+}$  and  $\beta 4\text{GalT-I}^{-/-}$  mice, we performed immunohistochemical staining with an anti-CD31 antibody (Figure 9; A to D). There was no difference in the vessel density of uninjured skin between the  $\beta 4\text{GalT-I}^{+/+}$  and  $\beta 4\text{GalT-I}^{-/-}$  mice (Figure 9E). Six days after the injury, the vascular density in the wound bed of  $\beta 4\text{GalT-I}^{-/-}$  mice was significantly lower than that of  $\beta 4\text{GalT-I}^{+/+}$

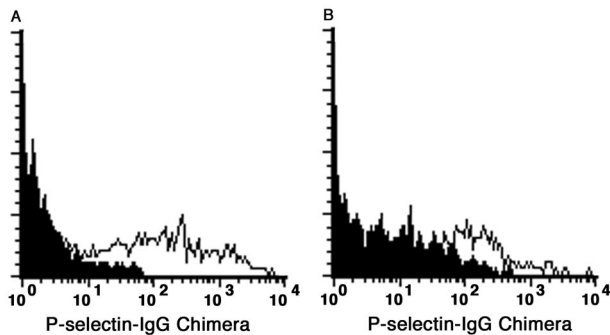


**Figure 6.** Binding of P-selectin to infiltrated neutrophils. Binding of the P-selectin-hlgG chimeric molecule to neutrophils (Gr-1 gated) infiltrated into wound sites 24 hours after the injury was analyzed by flow cytometry. Infiltrated neutrophils from  $\beta 4\text{GalT-I}^{+/+}$  (**A**) and  $\beta 4\text{GalT-I}^{-/-}$  (**B**) mice were stained with the P-selectin-hlgG (open histogram) and the second antibody (PE-anti-hlgG) alone (closed histogram). Representative results of three independent experiments are shown.

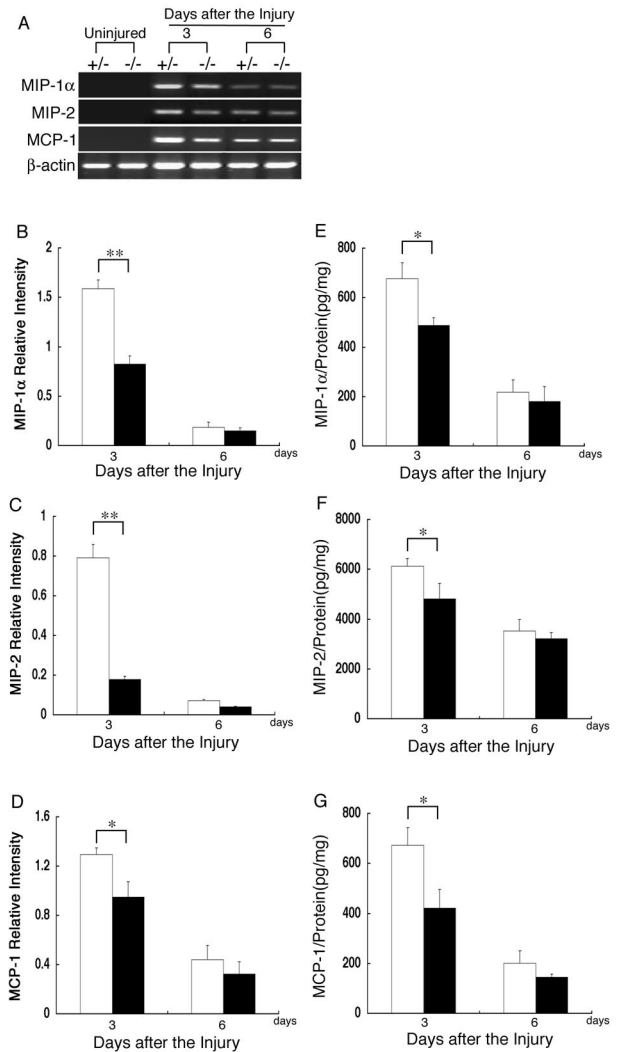


**Figure 7.** Expression of chemokines at wound sites. **A:** RT-PCR analysis of the gene expression of MIP-1 $\alpha$ , MIP-2, and MCP-1 at wound sites in  $\beta 4\text{GalT-I}^{+/+}$  and  $\beta 4\text{GalT-I}^{-/-}$  mice. RT-PCR analysis did not show any of these mRNAs in uninjured skin samples from mice of either genotype. Representative results of the six animals in each group are shown. Relative expression levels of MIP-1 $\alpha$  (**B**), MIP-2 (**C**), and MCP-1 (**D**) to  $\beta$ -actin in  $\beta 4\text{GalT-I}^{+/+}$  (open bars) and  $\beta 4\text{GalT-I}^{-/-}$  (filled bars) mice were determined by RT-PCR at 3 and 6 days after the injury. Data are expressed as the mean  $\pm$  SEM ( $n = 6$ ). \*,  $P < 0.05$ ; \*\*,  $P < 0.01$ . Protein levels of MIP-1 $\alpha$  (**E**), MIP-2 (**F**), and MCP-1 (**G**) in the wound sites of  $\beta 4\text{GalT-I}^{+/+}$  (open bars) and  $\beta 4\text{GalT-I}^{-/-}$  (filled bars) mice were analyzed by ELISA. Data are expressed as the mean  $\pm$  SEM ( $n = 6$ ). \*,  $P < 0.05$ ; \*\*,  $P < 0.01$ .

mice (1.8% in  $\beta 4\text{GalT-I}^{-/-}$  mice versus 4.2% in  $\beta 4\text{GalT-I}^{+/+}$  mice,  $P < 0.01$ ) (Figure 9E). The expression level of the VEGF gene, a major regulator of angiogenesis, was also assessed using semiquantitative RT-PCR analysis (Figure 9F). Although VEGF mRNA was strongly induced after the injury in both mice, its level 6 days after the injury was lower in the  $\beta 4\text{GalT-I}^{-/-}$  mice than in the  $\beta 4\text{GalT-I}^{+/+}$  mice (Figure 9G). The  $\beta 4\text{GalT-I}^{-/-}$  mice also showed significantly lower VEGF protein levels 6 days after the injury, compared with the  $\beta 4\text{GalT-I}^{+/+}$  mice, which correlated with the reduced mRNA levels (Figure 9H). These results indicate impaired angiogenesis in the  $\beta 4\text{GalT-I}^{-/-}$  mice in the proliferation phase of wound healing.



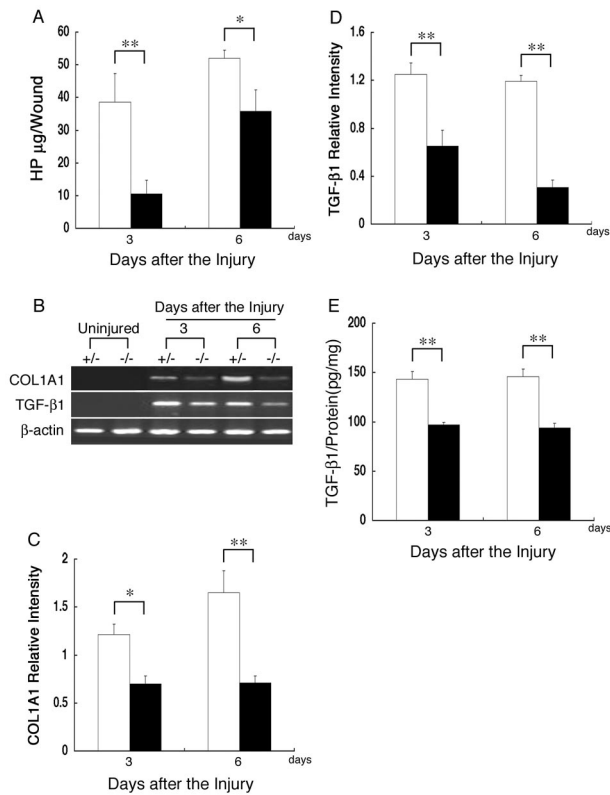


**Figure 8.** Collagen content at wound sites. **A:** Collagen content was assessed by quantitatively measuring the HP content of the wound sites of  $\beta 4$ GalT-I<sup>+/-</sup> (open bars) and  $\beta 4$ GalT-I<sup>-/-</sup> (filled bars) mice 3 and 6 days after the injury. Data are expressed as the mean  $\pm$  SEM ( $n = 6$ ). \*,  $P < 0.05$ ; \*\*,  $P < 0.01$ . **B:** RT-PCR analysis of the expression of COL1A1 and TGF- $\beta 1$  genes in the wound sites of  $\beta 4$ GalT-I<sup>+/-</sup> and  $\beta 4$ GalT-I<sup>-/-</sup> mice. Representative results of the six animals in each group are shown. Relative expression levels of COL1A1 (C) and TGF- $\beta 1$  (D) to  $\beta$ -actin in  $\beta 4$ GalT-I<sup>+/-</sup> (open bars) and  $\beta 4$ GalT-I<sup>-/-</sup> (filled bars) mice were determined by RT-PCR at 3 and 6 days after the injury. Data are expressed as the mean  $\pm$  SEM ( $n = 6$ ). \*,  $P < 0.05$ ; \*\*,  $P < 0.01$ . **E:** Protein levels of TGF- $\beta 1$  in wound samples from  $\beta 4$ GalT-I<sup>+/-</sup> (open bars) and  $\beta 4$ GalT-I<sup>-/-</sup> (filled bars) mice were analyzed by ELISA. Data are expressed as the mean  $\pm$  SEM ( $n = 6$ ). \*\*,  $P < 0.01$ .

## Discussion

There have been few reports of a biological role for carbohydrate chains in skin wound healing and this is the first report that shows a critical role for  $\beta 4$ -galactosylated carbohydrate chains in skin wound healing using genetically modified  $\beta 4$ GalT-I-deficient mice. The results obtained in this study revealed that wound closure was significantly delayed concomitant with reduced leukocyte infiltration at the wound site in  $\beta 4$ GalT-I<sup>-/-</sup> mice, indicating indispensable and cooperative roles for  $\beta 4$ -galactosylated carbohydrate chains in skin wound healing.

Skin injury immediately causes clot formation and local inflammation characterized by an infiltration of neutrophils and macrophages into the wound sites. These pathological changes are hallmarks of the inflammatory phase of wound healing.<sup>1,2</sup> The migration of neutrophils and macrophages into inflamed sites is closely related with cell adhesion through interaction between selectins and their ligands. Actually, P- and E-selectin double-deficient mice show an impaired infiltration of neutrophils and macrophages during wound healing, although single

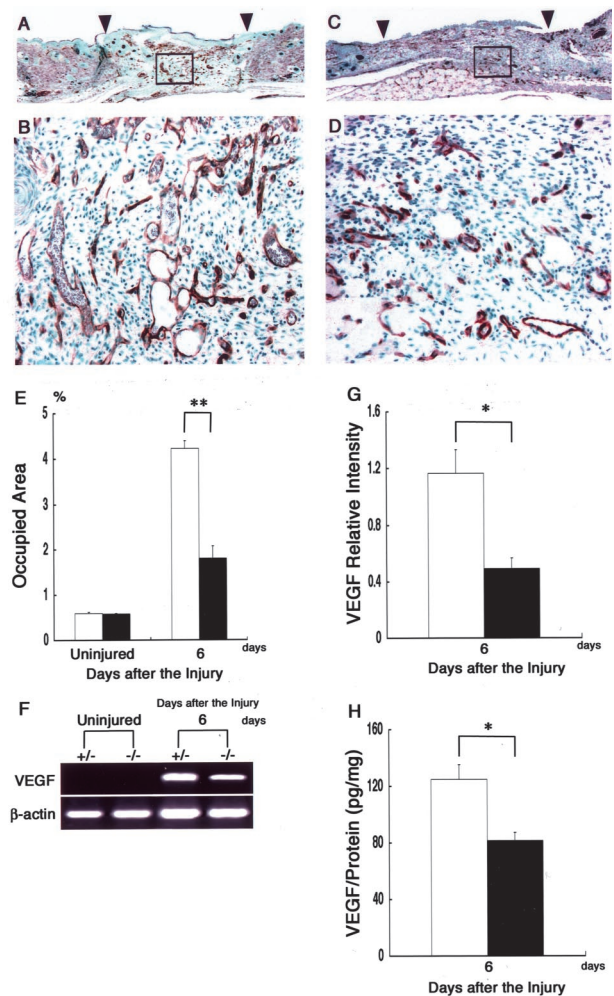


**Figure 9.** Analysis of angiogenesis at wound sites. **A to D:** Immunohistochemical sections of wound sites of  $\beta 4$ GalT-I<sup>+/-</sup> (A and B) and  $\beta 4$ GalT-I<sup>-/-</sup> (C and D) mice 6 days after the injury. Sections were stained with a monoclonal antibody for endothelium (CD31). Representative results from the six animals in each group are shown. **E:** The areas of the wound beds that were CD31-positive areas of  $\beta 4$ GalT-I<sup>+/-</sup> (open bars) and  $\beta 4$ GalT-I<sup>-/-</sup> (filled bars) mice were quantified using Photoshop software before and after the injury. Data are expressed as the mean  $\pm$  SEM ( $n = 6$ ). \*\*,  $P < 0.01$ . **F:** RT-PCR analysis of VEGF gene expression at the wound sites of  $\beta 4$ GalT-I<sup>+/-</sup> and  $\beta 4$ GalT-I<sup>-/-</sup> mice. RT-PCR did not show any VEGF mRNA in uninjured skin samples from mice of either genotype. Representative results from the six animals in each group are shown. **G:** Relative expression levels of VEGF to  $\beta$ -actin in  $\beta 4$ GalT-I<sup>+/-</sup> (open bar) and  $\beta 4$ GalT-I<sup>-/-</sup> (filled bar) mice were determined by RT-PCR 6 days after the injury. Data are expressed as the mean  $\pm$  SEM ( $n = 6$ ). \*,  $P < 0.05$ . **H:** VEGF protein levels in wound samples from  $\beta 4$ GalT-I<sup>+/-</sup> (open bar) and  $\beta 4$ GalT-I<sup>-/-</sup> (filled bar) mice were analyzed by ELISA. Data are expressed as the mean  $\pm$  SEM ( $n = 6$ ). \*,  $P < 0.05$ . Original magnifications:  $\times 20$  (A and C);  $\times 200$  (B and D).

mutant mice are not affected in leukocyte recruitment, except for an early decrease in neutrophil recruitment in P-selectin-deficient mice.<sup>19</sup> The reduced recruitment of keratinocytes together with the delayed migration of keratinocytes may cause the impaired wound healing in P- and E-selectin double-deficient mice. Moreover, the lack of  $\alpha$ -1,3-fucosyltransferase-VII or  $\beta 4$ GalT-I impairs the biosynthesis of selectin ligands such as sLe<sup>x</sup>, resulting in the attenuation of inflammatory responses.<sup>18,28</sup> Consistently, in the present study, the infiltration of neutrophils and macrophages into wound sites and the expression of P-selectin-ligands on the infiltrated neutro-

phils were impaired in  $\beta 4\text{GalT-I}^{-/-}$  mice. The infiltrated neutrophils expressed selectin ligands weakly in  $\beta 4\text{GalT-I}^{-/-}$  mice, probably because the biosynthesis of selectin ligands was attenuated, but not completely blocked, in  $\beta 4\text{GalT-I}^{-/-}$  mice as reported previously.<sup>18</sup> Taken together, these reports indicate that cell adhesion through selectins and carbohydrate selectin ligands is indispensable for leukocyte recruitment in the inflammatory phase of wound healing.

Accumulating evidence indicates the crucial involvement of chemokines as well as adhesion molecules in leukocyte infiltration. The present results demonstrate that the expression of several chemokines such as MIP-1 $\alpha$ , MIP-2, and MCP-1, which are chemoattractants for neutrophils and monocytes/macrophages,<sup>29</sup> were all reduced at the wound site of  $\beta 4\text{GalT-I}^{-/-}$  mice. The most likely reason for this reduction is that the number of neutrophils and macrophages recruited into the wound site was reduced because neutrophils and macrophages are major sources of these chemokines during skin wound healing (our unpublished data). Moreover, the reduced production of these chemokines might cooperatively cause further attenuation of leukocyte infiltration. On the other hand, wound repair, including re-epithelialization, angiogenesis, and collagen synthesis is delayed in MCP-1 $^{-/-}$  mice without any change in the level of macrophage recruitment into wound sites,<sup>21</sup> suggesting that MCP-1 regulates the effector state of macrophages and other cell types but not macrophage recruitment.

The inflammatory response is believed to be instrumental in supplying the growth factors, cytokines, and chemokines that orchestrate the cell movement necessary for wound repair.<sup>1,2</sup> Macrophages that have infiltrated into wounded tissues produce large amounts of these factors. In the re-epithelialization process, macrophages produce TGF- $\alpha$ , a key regulator of keratinocyte proliferation at the wound site.<sup>30</sup> The reduced expression of TGF- $\alpha$  mRNA, which was probably because of the reduced infiltration of macrophages in the wound site, might have caused the delayed re-epithelialization in the  $\beta 4\text{GalT-I}^{-/-}$  mice. TGF- $\beta 1$  and VEGF are a principal fibrogenic factor and a potent angiogenic factor in adult skin wound healing, respectively.<sup>31,32</sup> Thus, the reduced expression of TGF- $\beta 1$  and VEGF might result in the attenuation of collagen synthesis and angiogenesis in  $\beta 4\text{GalT-I}^{-/-}$  mice, respectively. Collectively, the delayed tissue granulation, including delays in collagen synthesis and angiogenesis, in the  $\beta 4\text{GalT-I}^{-/-}$  mice might be caused by the reduced number of activated macrophages that produce a variety of factors such as TGF- $\beta 1$  and VEGF necessary for tissue repair. The ultimate endpoint of the wound healing, however, was comparable between  $\beta 4\text{GalT-I}^{-/-}$  and  $\beta 4\text{GalT-I}^{+/-}$  mice, suggesting the early inflammatory phase of wound healing was affected.

An absence or a decrease in macrophage number at the wound sites impairs tissue repair,<sup>33</sup> and transfer of macrophages into aged mice accelerates wound healing.<sup>34</sup> Skin wound healing is impaired with decreased macrophage infiltration in mice deficient in interleukin-6 or ICAM-1.<sup>9,35</sup> In contrast, the depletion of neutrophils by

anti-neutrophil sera accelerates only re-epithelialization but not collagen contents and does not lead to delayed wound repair.<sup>36</sup> Thus, macrophage recruitment is considered to be important for wound healing. Therefore, a possible explanation for the delayed wound repair in the  $\beta 4\text{GalT-I}^{-/-}$  mice could be the impaired macrophage infiltration in the inflammatory phase. However, several recent reports have raised questions on the validity of this notion. Skin wounds are healed in the neonate PU.1-null macrophageless mice with the same time course as in wild-type littermates, implying that wound repair of neonates is not dependent on inflammatory cells.<sup>37</sup> Secretory leukocyte protease inhibitor-deficient mice exhibit impaired wound healing despite or because of exaggerated leukocyte infiltration into wound sites.<sup>38</sup> Skin wound healing is accelerated despite reduced leukocyte infiltration in mice deficient in Smad3 or TNF-Rp55.<sup>8,39</sup> Collectively, in an aseptic wound model, the regulation of macrophage-derived growth factors that are responsible for re-epithelialization, angiogenesis, and collagen synthesis may be more important than the quantity of recruited macrophages. Most of the factors that regulate wound healing are glycoproteins, and their glycosylation patterns affect their biological activity, stability, transport, and clearance from the circulation.<sup>40</sup> We cannot rule out the possibility that impaired glycosylation of any of the crucial chemokines, cytokines, growth factors, or of their receptors might cause the delayed wound healing in the  $\beta 4\text{GalT-I}^{-/-}$  mice.

A human hereditary disease, leukocyte adhesion deficiency (LAD), is caused by immunodeficiency owing to the defective adhesion of leukocytes to the endothelial cell surface. LAD-I patients possess mutations in the  $\beta 2$  integrin gene, and LAD-II (also known as congenital disorders of glycosylation (CDG)-IIc) patients have impaired selectin ligand biosynthesis owing to mutations in the GDP-fucose transporter gene.<sup>41-43</sup> These LAD patients suffer from severe bacterial infection and impaired wound healing.<sup>44,45</sup> A human mutation in the  $\beta 4\text{GalT-I}$  gene has recently been identified in an infant boy with mental retardation, hydrocephalus, myopathy, and blood-clotting defects, and designated as CDG-IIId.<sup>46</sup> Because only a single infant patient has been identified to date, and only a few biochemical parameters were analyzed in that patient,<sup>47</sup> it is still unknown whether the human mutation in the  $\beta 4\text{GalT-I}$  gene causes the selectin ligand deficiency, impaired wound healing, and inflammatory responses we observed in the mouse.

In summary, our data demonstrate that  $\beta 4$ -galactosylated carbohydrate chains synthesized by  $\beta 4\text{GalT-I}$  play a critical role in skin wound healing. In particular, the impaired leukocyte infiltration in the inflammatory phase that is probably because of the defect in selectin-ligand biosynthesis could result in the delayed wound healing we observed in the  $\beta 4\text{GalT-I}^{-/-}$  mice. The  $\beta 4\text{GalT-I}^{-/-}$  mouse could be a good animal model of CDG-IIId syndrome and mimic some symptoms of CDG-IIc patients, who are deficient in selectin-ligand biosynthesis. Further analysis of  $\beta 4\text{GalT-I}^{-/-}$  mice may lead to good therapies for skin wound healing and CDG syndromes.

## Acknowledgments

We thank Dr. S. Shibata, Dr. Y. Sato (Kanazawa University), and Ms. Y. Ishida (Wakayama Medical University) for valuable comments regarding the FACS analysis, histological analysis, and ELISA; and all the members of the Division of Transgenic Animal Science (Kanazawa University) for excellent animal care.

## References

- Martin P: Wound healing—aiming for perfect skin regeneration. *Science* 1997, 276:75–81
- Singer AJ, Clark RA: Cutaneous wound healing. *N Engl J Med* 1999, 341:738–746
- Keane MP, Strieter RM: The role of CXC chemokines in the regulation of angiogenesis. *Chem Immunol* 1999, 72:86–101
- Campbell JJ, Butcher EC: Chemokines in tissue-specific and micro-environment-specific lymphocyte homing. *Curr Opin Immunol* 2000, 12:336–341
- Rossi D, Zlotnik A: The biology of chemokines and their receptors. *Annu Rev Immunol* 2000, 18:217–242
- Sallusto F, Mackay CR, Lanzavecchia A: The role of chemokine receptors in primary, effector, and memory immune responses. *Annu Rev Immunol* 2000, 18:593–620
- Seeger S, Nelson PJ, Schlondorff D: Chemokines, chemokine receptors, and renal disease: from basic science to pathophysiological and therapeutic studies. *J Am Soc Nephrol* 2000, 11:152–176
- Mori R, Kondo T, Ohshima T, Ishida Y, Mukaida N: Accelerated wound healing in tumor necrosis factor receptor p55-deficient mice with reduced leukocyte infiltration. *FASEB J* 2002, 16:963–974
- Lin ZQ, Kondo T, Ishida Y, Takayasu T, Mukaida N: Essential involvement of IL-6 in the skin wound-healing process as evidenced by delayed wound healing in IL-6-deficient mice. *J Leukoc Biol* 2003, 73:713–721
- Amado M, Almeida R, Schwientek T, Clausen H: Identification and characterization of large galactosyltransferase gene families: galactosyltransferases for all functions. *Biochim Biophys Acta* 1999, 1473:35–53
- Hennet T: The galactosyltransferase family. *Cell Mol Life Sci* 2002, 59:1081–1095
- McEver RP, Moore KL, Cummings RD: Leukocyte trafficking mediated by selectin-carbohydrate interactions. *J Biol Chem* 1995, 270:11025–11028
- Lowe JB: Selectin ligands, leukocyte trafficking, and fucosyltransferase genes. *Kidney Int* 1997, 51:1418–1426
- Asano M, Furukawa K, Kido M, Matsumoto S, Umesaki Y, Kochibe N, Iwakura Y: Growth retardation and early death of  $\beta$ -1,4-galactosyltransferase knockout mice with augmented proliferation and abnormal differentiation of epithelial cells. *EMBO J* 1997, 16:1850–1857
- Lu Q, Hasty P, Shur BD: Targeted mutation in  $\beta$ 1,4-galactosyltransferase leads to pituitary insufficiency and neonatal lethality. *Dev Biol* 1997, 181:257–267
- Lu Q, Shur BD: Sperm from  $\beta$ 1,4-galactosyltransferase-null mice are refractory to ZP3-induced acrosome reactions and penetrate the zona pellucida poorly. *Development* 1997, 124:4121–4131
- Steffgen K, Dufraux K, Hathaway H: Enhanced branching morphogenesis in mammary glands of mice lacking cell surface  $\beta$ 1,4-galactosyltransferase. *Dev Biol* 2002, 244:114–133
- Asano M, Nakae S, Kotani N, Shirafuji N, Nambu A, Hashimoto N, Kawashima H, Hirose M, Miyasaka M, Takasaki S, Iwakura Y: Impaired selectin-ligand biosynthesis and reduced inflammatory responses in  $\beta$ -1,4-galactosyltransferase-I-deficient mice. *Blood* 2003, 102:1678–1685
- Subramaniam M, Saffaripour S, Van De Water L, Frenette PS, Mayadas TN, Hynes RO, Wagner DD: Role of endothelial selectins in wound repair. *Am J Pathol* 1997, 150:1701–1709
- Kotani N, Asano M, Iwakura Y, Takasaki S: Knockout of mouse  $\beta$ 1,4-galactosyltransferase-1 gene results in a dramatic shift of outer chain moieties of N-glycans from type 2 to type 1 chains in hepatic membrane and plasma glycoproteins. *Biochem J* 2001, 357:827–834
- Low QE, Drugea IA, Duffner LA, Quinn DG, Cook DN, Rollins BJ, Kovacs EJ, DiPietro LA: Wound healing in MIP-1a<sup>-/-</sup> and MCP-1<sup>-/-</sup> mice. *Am J Pathol* 2001, 159:457–463
- Nakae S, Naruse-Nakajima C, Sudo K, Horai R, Asano M, Iwakura Y: IL-1 alpha, but not IL-1 beta, is required for contact-allergen-specific T cell activation during the sensitization phase in contact hypersensitivity. *Int Immunol* 2001, 13:1471–1478
- Woessner J: The determination of hydroxyproline in tissue and protein samples containing small proportions of the imino acid. *Arch Biochem Biophys* 1961, 93:440–447
- Schrier DJ, Phan SH, McGarry BM: The effects of the nude (nu/nu) mutation on bleomycin-induced pulmonary fibrosis. A biochemical evaluation. *Am Rev Respir Dis* 1983, 127:614–617
- Yokoi H, Natsuyama S, Iwai M, Noda Y, Mori T, Mori KJ, Fujita K, Nakayama H, Fujita J: Non-radioisotopic quantitative RT-PCR to detect changes in mRNA levels during early mouse embryo development. *Biochem Biophys Res Commun* 1993, 195:769–775
- Nakayama H, Yokoi H, Fujita J: Quantification of mRNA by non-radioactive RT-PCR and CCD imaging system. *Nucleic Acids Res* 1992, 20:4939
- Austyn JM, Gordon S: F4/80, a monoclonal antibody directed specifically against the mouse macrophage. *Eur J Immunol* 1981, 11:805–815
- Maly P, Thall A, Petryniak B, Rogers CE, Smith PL, Marks RM, Kelly RJ, Gersten KM, Cheng G, Saunders TL, Camper SA, Camphausen RT, Sullivan FX, Isogai Y, Hinds Gaul O, von Andrian UH, Lowe JB: The  $\alpha$ (1,3)fucosyltransferase Fuc-TVII controls leukocyte trafficking through an essential role in L-, E-, and P-selectin ligand biosynthesis. *Cell* 1996, 86:643–653
- Nelson PJ, Krensky AM: Chemokines, chemokine receptors, and allograft rejection. *Immunity* 2001, 14:377–386
- Rappolee DA, Mark D, Banda MJ, Werb Z: Wound macrophages express TGF- $\alpha$  and other growth factors in vivo: analysis by mRNA phenotyping. *Science* 1988, 241:708–712
- Frank S, Madlener M, Werner S: Transforming growth factors  $\beta$ 1,  $\beta$ 2, and  $\beta$ 3 and their receptors are differentially regulated during normal and impaired wound healing. *J Biol Chem* 1996, 271:10188–10193
- Ozawa K, Kondo T, Hori O, Kitao Y, Stern DM, Eisenmenger W, Ogawa S, Ohshima T: Expression of the oxygen-regulated protein ORP150 accelerates wound healing by modulating intracellular VEGF transport. *J Clin Invest* 2001, 108:41–50
- Leibovich SJ, Ross R: The role of the macrophage in wound repair. A study with hydrocortisone and antimacrophage serum. *Am J Pathol* 1975, 78:71–100
- Danon D, Kowatch MA, Roth GS: Promotion of wound repair in old mice by local injection of macrophages. *Proc Natl Acad Sci USA* 1989, 86:2018–2020
- Nagaoka T, Kaburagi Y, Hamaguchi Y, Hasegawa M, Takehara K, Steeber DA, Tedder TF, Sato S: Delayed wound healing in the absence of intercellular adhesion molecule-1 or L-selectin expression. *Am J Pathol* 2000, 157:237–247
- Dovi JV, He LK, DiPietro LA: Accelerated wound closure in neutrophil-depleted mice. *J Leukoc Biol* 2003, 73:448–455
- Martin P, D'Souza D, Martin J, Grose R, Cooper L, Maki R, McKercher SR: Wound healing in the PU. 1 null mouse—tissue repair is not dependent on inflammatory cells. *Curr Biol* 2003, 13:1122–1128
- Ashcroft GS, Lei K, Jin W, Longenecker G, Kulkarni AB, Greenwell-Wild T, Hale-Donze H, McGrady G, Song XY, Wahl SM: Secretory leukocyte protease inhibitor mediates non-redundant functions necessary for normal wound healing. *Nat Med* 2000, 6:1147–1153
- Ashcroft GS, Yang X, Glick AB, Weinstein M, Letterio JL, Mizel DE, Anzano M, Greenwell-Wild T, Wahl SM, Deng C, Roberts AB: Mice lacking Smad3 show accelerated wound healing and an impaired local inflammatory response. *Nat Cell Biol* 1999, 1:260–266
- Gagneux P, Varki A: Evolutionary considerations in relating oligosaccharide diversity to biological function. *Glycobiology* 1999, 9:747–755
- Kishimoto TK, Hollander N, Roberts TM, Anderson DC, Springer TA: Heterogeneous mutations in the beta subunit common to the LFA-1, Mac-1, and p150,95 glycoproteins cause leukocyte adhesion deficiency. *Cell* 1987, 50:193–202
- Luhn K, Wild MK, Eckhardt M, Gerardy-Schahn R, Vestweber D: The



- gene defective in leukocyte adhesion deficiency II encodes a putative GDP-fucose transporter. *Nat Genet* 2001, 28:69–72
43. Lubke T, Marquardt T, Etzioni A, Hartmann E, von Figura K, Korner C: Complementation cloning identifies CDG-IIc, a new type of congenital disorders of glycosylation, as a GDP-fucose transporter deficiency. *Nat Genet* 2001, 28:73–76
  44. Anderson DC, Schmalsteig FC, Finegold MJ, Hughes BJ, Rothlein R, Miller LJ, Kohl S, Tosi MF, Jacobs RL, Waldrop TC, Grolman AS, Shearer WT, Springer TA: The severe and moderate phenotypes of heritable Mac-1, LFA-1 deficiency: their quantitative definition and relation to leukocyte dysfunction and clinical features. *J Infect Dis* 1985, 152:668–689
  45. Roos D, Law SK: Hematologically important mutations: leukocyte adhesion deficiency. *Blood Cells Mol Dis* 2001, 27:1000–1004
  46. Hansske B, Thiel C, Lubke T, Hasilik M, Honing S, Peters V, Heidemann PH, Hoffmann GF, Berger EG, von Figura K, Korner C: Deficiency of UDP-galactose:N-acetylglucosamine  $\beta$ -1,4-galactosyltransferase I causes the congenital disorder of glycosylation type IIc. *J Clin Invest* 2002, 109:725–733
  47. Peters V, Penzien JM, Reiter G, Korner C, Hackler R, Assmann B, Fang J, Schaefer JR, Hoffmann GF, Heidemann PH: Congenital disorder of glycosylation IIc (CDG-IIc)—a new entity: clinical presentation with Dandy-Walker malformation and myopathy. *Neuropediatrics* 2002, 33:27–32